

# Production of Electricity and Improved Conversion Efficiency By Using Ionic Liquid in Photogalvanic Cell

Samar H. Bendary (✉ [samar.epri90@gmail.com](mailto:samar.epri90@gmail.com))

Egyptian Petroleum Research Institute <https://orcid.org/0000-0001-9458-7276>

Mohamed A. Betiha

Egyptian Petroleum Research Institute

Sawsan A. Mahmoud

Egyptian Petroleum Research Institute

---

## Research Article

**Keywords:** photogalvanic cell, Ionic Liquid, Conversion Efficiency, Storage Capacity

**Posted Date:** February 10th, 2021

**DOI:** <https://doi.org/10.21203/rs.3.rs-172564/v1>

**License:**   This work is licensed under a Creative Commons Attribution 4.0 International License.

[Read Full License](#)

---

# Abstract

Surfactant were widely applied in photogalvanic cells (PGC), and a limited number of studies have reported to used ionic liquid (IL), although it has more advantages than the conventional surfactants due to their specific chemical and physical properties such as the high electrolytic properties, the strong hydrophobic interactions between  $C_n\text{mim}^+$  and hydrophobic portion of other surfactant and co-surfactant behavior. In this work, Synthesis of IL Diethyl ammonium tetrachloro ferrate (DATF) was done through two step method. The composition of the produced IL was investigated by FTIR and  $^1\text{H}$ NMR spectra techniques. IL was known as a salt in the liquid state or a salt with melting point below the boiling point of water. PGC can be described as an electrochemical cell, where the change in both voltage and current results from photochemically generated changes in the proportional concentrations of the reactants during the oxidation-reduction reaction in the cell. The present study has shown electrical cell performance of the PGC as  $P_{PP}$  96.2 $\mu$ W,  $i_{SC}$  370  $\mu$ A,  $V_{OC}$  650 mV,  $\eta$  1.9 %, and  $t_{0.5}$  105 minutes, for PGC system containing Tris (2,2'-bipyridyl) Ruthenium (II) chloride hexahydrate (TBRC) as photosensitize, Oxalic acid (OX) as reductant and (DATF) as IL under artificial and low illumination intensities, this system not yet reported in the literature. The study of variation of the different cell parameters has shown optimum cell performance at an optimal value of these cell fabrication parameters, and a preliminary mechanism for the production of energy in PGC was also proposed.

## Introduction

Fossil fuels are the primary source of energy in the world and feed most of modern civilization as we know it, from transportation to industrial applications, but this model will not last forever. Humans have used fuels in abundant quantities since the nineteenth century and if consumption continues at this rate, fuel resources will be depleted more quickly than the rate of formation. Also, technological progress and overpopulation constitute a significant risk to the global fuel reserve, as studies indicate that demand for consumption will increase by 53 percent during 2030 [1]. Therefore, it is necessary to search for new sources to meet the needs of the world during the coming years.

in 2017, solar energy accounted for 1.7% of electricity production in the world, and it is growing at a rate of 35% every year. [2]. General solar energy can easily be converted to electricity [3] through multiple different types of solar cells such as photovoltaic cells (PV), dye sensitized solar cells (DSSC) [4-6], perovskite cells (PRC), polymer cells (PC) and (PGC) [7]. The PGC effect as “the change in the electrode potential of a galvanic system, produced by illumination and traceable to a photochemical process in the body of the electrolyte” was described by Rabinowitch [8, 9].

The most important characteristic of galvanic cells (PG) is their ability to store energy compared to other types of solar cells (in theory 18%, but the actual value is much lower) [10, 11]. Therefore, in the recent period, research focused on how to treat and develop each component of the cell i.e., reductants, electrolyte and photosensitizers in order to raise the conversion efficiency [10].

IL one of the main components of PGC, and can be defined as salt that are primarily composed of organic cations and organic or inorganic anions the cationic segment of IL includes alkyl-subbed imidazolium, pyrrolidinium, piperidinium, ammonium, phosphonium, sulfonium and the anionic part includes halide, BF<sub>4</sub>, PF<sub>6</sub>, Cl, Br, thiocyanate, and di sulfonyl imide.

Often difficult to determine the melting point of this compound since they are considered to be “notorious” glass-forming materials these compounds are characterized by a very wide liquid range due to the wide temperature range between the melting point and boiling point [12]. Because of the chemical composition of IL which consists of an organic cation and inorganic polyatomic anion; thus, their potential numbers are enormous and cannot be limited. Therefore, innovation and development in the methods of preparation and determining its components and characteristics is a major challenge among scientists. In 1914 the IL was first prepared using ethyl ammonium nitrate and is considered the starting point for what is known as the IL [12]. IL have been extensively applied to photovoltaic cells, but their application is limited to photo galvanic cells [13-21]. Plentiful studies of PGC were monitored [22–27], as they dealt with the change in the cell components from photosensitizers to reductants.

To our best review study, no one has paid attention to correlate the electrical output of PGC with IL, which plays an influential role in the efficiency. Therefore, in present work, DATF was prepared and studied as a substitute for surfactant, and mixed with OX as a reducing agent and TBRC as photosensitizer to improve the conversion efficiency of solar cells to electricity.

## Experimental

### 2.1 Materials

TBRC, OX, were used as the photo-sensitizer and reductant, Di ethylamine, Iron (III) chloride hexahydrate and Di ethyl ether, Aldrich. Hydrochloric acid, Adwic, Egypt, were used. All solutions were prepared with distilled water and preserved in dark containers and kept in the dark to shield them from sunlight. After preparing the desired solutions to be applied in PGC, it is poured into a H tube glass and keep the PH of the cell in the acidic medium. The next step is submerging the platinum electrode in one arm (illuminated) and saturated calomel electrode (SCE) in the other arm (dark) of the cell and connect them to the microammeter. finally, at the first PGC was set in dark until stable potential was accomplished then the light source is shed on the platinum electrode.

to cut any thermal radiation a water filter was used. The photochemical of the photosensitizer was concentrated potentiometrically. An advanced pH meter (HANNA Model-212) and a microammeter (Extech EX420 Autoranging) were utilized to gauge the electrical yield from photopotential and photocurrent. The H-type tube with the electrical associations and key, Figure 1 shows the cell structure and mechanism of operation.

### 2.2. Synthesis of DATF

First, Di ethyl ammonium chloride was prepared according to the following procedure: One mole of di ethylamine was stirred with 1.1 mole of hydrochloric acid for 2 h at 50 °C. The resultant di ethylamine hydrochloride was washed several times with di ethyl ether to remove unreacted amine. Secondly, DATF was synthesized by mixing equimolar amounts of Di ethyl ammonium chloride and  $\text{FeCl}_3 \cdot 6\text{H}_2\text{O}$  under  $\text{N}_2$  gas for 24 h at 60 °C. The product formed from DATF Figure 2, was washed with diethyl ether and distilled water several times, finally it was dried in vacuum at 60°C for 2h [28].

## Results And Discussion

### 3.1. Chemical structure confirmation of the synthesized compound:

#### 3.1.1. FTIR spectra

Fig. 3a showed the FTIR spectrum of DATF. The appearance of characteristic bands at  $2850.88\text{cm}^{-1}$  and  $2920.68\text{cm}^{-1}$  due to the presence of (CH symmetric stretching) and (CH asymmetric stretching), respectively, two vibrational bands at  $1470.64\text{cm}^{-1}$ ,  $1392.53\text{cm}^{-1}$  due to the presence of ( $\text{CH}_3$  and  $\text{CH}_2$  asymmetric bending). The appearance of vibrational band at  $2521.21\text{cm}^{-1}$  due to the presence of ( $\text{NH}_2$  asymmetric stretching) and the appearance of a vibrational band at  $1602.79\text{cm}^{-1}$  due to ( $\text{NH}_2$  asymmetric bending).

#### 3.1.2. $^1\text{H}$ NMR spectra

Fig. 3b showed  $^1\text{H}$ -NMR ( $\text{DMSO-d}_6$ ) spectrum of DATF. different peaks were observed at  $\delta=1.1\text{ppm}$  (t, 6H,  $(\text{CH}_3)_2$ );  $\delta=3.2\text{ppm}$  (q, 4H,  $(\text{CH}_2)_2$ );  $\delta=7.9\text{ppm}$  (s, 2H,  $\text{NH}_2$ ).

#### 3.1.2. Performance of PGC

To determination of the voltage-current curve in the PGC, the results of the voltage and current are recorded by putting the PGC in the dark while keeping the circuit open until stable potential is achieved, the Pt electrode is exposed to the light from tungsten lamp. The water filter is placed between the cell and the lamp to cut off the infrared which could negatively affects the cell, and leads to decrease the performance. Upon illumination, the photovoltaic voltage (V) and the photocurrent (i) are generated by the system. After cell charging, the cell parameters such as maximum voltage ( $V_{\text{max}}$ ), open circuit potential ( $V_{\text{oc}}$ ), maximum current ( $i_{\text{max}}$ ), equilibrium balance ( $i_{\text{eq}}$ ) or short circuit current ( $i_{\text{sc}}$ ) are measured. I-V curve was obtained by registering different data of the voltage by changing the resistance value so that the potential current data are obtained until the value of the zero-current reached. The curve study shows the highest amount by which the cell can be used. The cell is operated at highest power (i.e., power at power point  $P_{\text{pp}}$ ) at corresponding external load, current (i.e., current at power point  $i_{\text{pp}}$ ) and potential (i.e., potential at power point  $V_{\text{pp}}$ ) in order to study its performance by monitoring the change in current and potential with time. After establishing the J-V curve and recording the result product the fill factor and conversion efficiency were calculated.

Fill factor is defined as the ratio of the maximum (actual) energy that can be obtained from solar cells to the (theoretic) value Eq (1).

While conversion efficiency known as the ability to convert the amount of forthcoming solar radiation from sun to electricity Eq (2). Both can be expressed as follow:

$$FF = \frac{V_{pp} \times I_{pp}}{V_{oc} \times J_{sc}} \quad (1)$$

$$\eta \% = \frac{V_{pp} \times I_{pp}}{10.4 \text{mW cm}^{-2} \times A} \times 100\% \quad (2)$$

Where ( $V_{pp}$  i.e., potential at power point), ( $I_{pp}$  i.e., current at power point) and ( $A$ ) is the area of Pt electrode.

The PGC charges were studied in a PGC system and the effects of different variables were discussed in order to achieve the highest conversion efficiency, eg; the variation in the pH values of the solution, and variation in the concentration of TBRC, DATF and OX.

### 3.2. Impact of the variety of pH

Initially, the variation in the pH has been studied in acid and alkali ranges. From this study the highest output of the cell was observed in the acidic medium and that by increasing the acidity the conversion efficiency increases to a certain extent and then decreases thereafter as we go to the alkaline medium.

In previous studies carried out by both Gangotri and Gangotri [29], Genwa and Chouhan [30], and Dube et al. [31], they recorded that the pH of the ideal condition is related with pKa of the reductant, where it is equal to or slightly higher than pKa of the reducing substance. These authors prescribe that the conceivable explanation behind this as the accessibility of the reductant in its in its neutral or anionic form a superior electron donor

From (Table 1 &Figure 4) it was observed that the maximum cell outputs from (photovoltaic power, photoelectric current, power at the power point, fill factor and conversion efficiency) were obtained in an acid medium at pH 2.5 and any increase after that leads to a significant reduce in the cell performance, this may be due to the fact with decrease pH hydrogen ion concentration increase protonation of dye occur with charge transfer and with pH increase complex may join with the oxidized state of the OX reductant, prohibit regeneration of its original state.

### 3.3. Impact of the variety in the concentration of TBRC

The photochemistry of dye is playing a significant role for understanding the mechanism of electron transfer reactions in photoelectrochemical devices such as PGC. The dye  $[\text{Ru}(\text{bpy})_3]^{2+}$  is considered an ideal dye, as it absorbs both visible and ultraviolet light. UV absorption ranges were observed at 285 nm

corresponding to concentrated ligand  $\pi\text{-}\pi^*$  transitions and a weak transition around 350 nm (d-d transition) as shown in figure 5 [32]. The results of light absorption in the formation of an excited state have a relatively long lifetime of 890 ns in acetonitrile and 650 ns seconds in water [33]. The excited state unwinds to the ground state by emitting a photon or non-radiative relaxation. Studies have shown that long lifetime of the excited state is due to being triple while the ground state is a single case due to the fact that the molecule allows separation of the charge. Most of the time, triple state transformations are prohibited, and therefore as slow, such as all molecular excitatory states. The triple excited state of  $[\text{Ru}(\text{bpy})_3]^{2+}$  is characterized by strong oxidizing properties and reduction compared to its ground state.



There are numerous derivatives from  $[\text{Ru}(\text{bpy})_3]^{2+}$  [34-38] and most of them have been applied in many different fields, including bio diagnostics, solar cell and organic light-emitting diode.

$[\text{Ru}(\text{bpy})_3]$  has been applied as a light sensitive dye in solar cells and has proven its efficiency due to its unique properties such as its chemical stability in aqueous solution, strong luminescence, good electrochemical Reversibility, moderate excited-state lifetime, electron transfer reactions, energy and chemical stability [39,40].

(Table 2 & Figure 6) was observed that the maximum cell outputs from (photovoltaic power, photoelectric current, power at the power point, fill factor and conversion efficiency) were obtained at  $4.1 \times 10^{-4}$  M and any increase or decrease after that leads to a significant reduce in the cell performance, this may be due to a low concentration of the dye, there is a restricted number of Photosensitizer atoms expected to ingest photons and give an electron to the Pt electrode in the cell, so there is a decrease in the cell's output, while higher concentration of photosensitizers doesn't allow the ideal light intensity to arrive at the particles close to the electrodes and thus, there was relating fall in the power of the cell.

### 3.4. Impact of the variety in the concentration of DATF

Thirdly, to improve the exhibition of the PGC, IL was applied as electrolytes, these salts have dissolving close toward room temperature and show properties of super cooled liquids whenever warmed over their melting point. PGC containing (DATF) electrolytes, was mix with the ruthenium-based sensitizer (Table 3 & Fig. 7) show an effectiveness up to 1.9% at  $10.4 \text{ mW/cm}^2$  also note that it is relatively stable in the long term. The variation in the concentration of DATF has been studied in low and high ranges. From (Table 3 and Figure 7) it was noted that the maximum cell output from (photoelectric energy, photoelectric current, energy at the power point, filling factor and conversion efficiency) were obtained at concentration of  $6 \times 10^{-2}$  M and any increase or decrease after that leads to significant decrease in cell performance, the reason for this may be due to when applying a low concentration there are a limited number of IL molecules available to transfer the electron and solubility of the Ruthenium dye, On the other hand, the

high concentration of the IL molecules works to impede the movement of the dye molecules on their way to the electrode, thus resulting in a decrease in the output energy. Also, the reason for the decrease in cell output may be due to potential problems caused by liquid organic electrolytes, such as organic solvent volatilization and leakage that had the effect of limiting long-term performance and practical use of dye-sensitized solar cells (DSSCs).

### **3.5. Impact of the variety in the concentration of OX**

Finally, OX is used in PGC as a (reducing agent) where an electron is lost in the chemical reaction to be received by another electron (oxidizing agent) in the oxidation reduction reaction. The effect of variation in the concentration of OX has been studied in low and high ranges. From (Table 4 & Figure 8) it was observed that the maximum cell outputs from (photovoltaic power, photoelectric current, power at the power point, fill factor and conversion efficiency) were obtained at concentration of  $1.9 \times 10^{-3} \text{M}$  and any increase or decrease after that leads to Significant decrease in cell performance, this may be due to the fact that at a low concentration of acid, the number of reducing agents' molecules in the solution decreases, thus the number of electrons that donate to the excited molecules of ruthenium dye decreases. While the high concentration of reducing agents can impede the motion of the ruthenium molecules in the solution from reaching across to the electrodes at the required time, on the other hand, it may also boost back electron transfer from the ruthenium particles to the OX reductant particles.

### **4. (I–V) characteristics of the cell**

The open circuit voltage  $V_{oc}$  and short circuit current  $i_{sc}$  of all these systems were measured with the help of a digital pH meter (keeping the other circuit open) and from a microammeter (keeping the other circuit closed), respectively. The electrical parameters in between these two extreme values ( $V_{oc}$  and  $i_{sc}$ ) were determined with the help of a carbon pot (log 470K) connected in the circuit of microammeter, through which an external load in the circuit was applied. After studying a series of variables on the galvanic cells, the highest outputs were recorded for PGC containing ( $4.1 \times 10^{-4} \text{M}$  of TBRC,  $2.5 \times 10^{-3} \text{M}$  of SDBS,  $1.9 \times 10^{-3} \text{M}$  of OX at pH 2.5, Pt electrode of area  $0.5 \text{cm}^2$  and light intensity =  $10.4 \text{mW cm}^{-2}$ ). The Figure 9 shows that potential increases with decreases in the current. The current and power data and curve is also shown in Table 5, and Figure 9. The maxima of this curve show the power at power point of the cell and in this system, it is  $96.2 \mu\text{W}$ . And, the current at power point ( $i_{pp}$ ) and potential at power point ( $V_{pp}$ ) for this PGC system is  $260 \mu\text{A}$  and  $370 \text{mV}$ , respectively.

### **5. Recover the amount of energy stored from solar cells in the dark (performance of the cell in the dark)**

Initially, the cell is charged in sunlight or any other light source until the cell reaches the highest possible energy then the light source is removed and the cell is placed in the dark. The stored energy is recovered from the cell in the dark as the time it takes for the energy to drop to half of its initial value is called  $t_{0.5}$ .

To assess the photo galvanic cell ability to store potential energy, energy recovery of its store in the dark was studied, as it was observed that the value of recovered energy decreased over time until it was fully

discharged. During the study, it was observed that the energy does not decrease quickly, but it decreases slowly and sometimes it stabilizes for several minutes, as shown in Figure 10. We note that the energy drops to half (48.1  $\mu\text{W}$ ) of its initial value (96.2  $\mu\text{W}$ ) at 105 minutes.

## 6. Stability tests of DATF system

A long-term stability test was performed for PGC with  $1.4 \times 10^{-4}$  M of TBRC as photosensitized with DATF  $6 \times 10^{-2}$  M as IL and  $1.9 \times 10^{-3}$  M of OX as reductant, at 0.5 active area of Pt and light intensity = 10.4  $\text{mWcm}^{-2}$ , which showed that the DSSC was stable for 10 day under full sunlight intensity.

The values changed over time for  $V_{\text{OC}}$ ,  $J_{\text{SC}}$ , FF and  $\eta$ , and are plotted in Figure 11. The initial parameters ( $V_{\text{OC}}$ ,  $J_{\text{SC}}$ , FF, and  $\eta$ ) are 650 mV, 370  $\mu\text{A}$ , 0.4, and 1.9%, respectively. During the test period for initial 3 days all parameters were stable, next three days  $V_{\text{OC}}$  increased slightly to reach 655, and decreased slightly to 643 mV by the end of the test, which is only 7 mV lower than the initial value (650 mV), indicating the good adsorption stability PGC system.

While  $I_{\text{SC}}$  exhibited a slightly decreasing to reach 364  $\text{mAcm}^{-2}$  and finally reached 360  $\mu\text{A}$  at the end of the test (10 day) which may originate from slow TBRC degradation. The  $\eta$  of the device slowly degraded to 1.7%, remaining at 90% of the initial value after 10 day of visible-light absorption. The high stability of the cell indicated that the TBRC had excellent stability with IL and that the degradation was insignificant.

## Conclusion

PGC<sub>s</sub> are more useful and economical compared to other solar cells like fuel cells, silicon cells, etc. The most important thing that distinguishes PGC from others is its superior ability to store energy by converting it into electrical energy, the ability to charge in very dim light, the ability to recover stored energy directly from the cell, and finally the ability to manufacture photovoltaics at the lowest possible cost and with the simplest technologies as mentioned previously. DATF has been prepared and applied as an alternative to surfactants, and has proven effective in converting solar energy into electrical energy. PGC consisting of DATF as IL, TBRC as photosensitivity, and OX as reducing agent were recorded with higher conversion efficiency and storage capacity 1.9%, and  $t_{0.5} = 105$  min compared to systems that used IL in PGC [41]. To some extent, this simple system can be used to overcome a power problem.

## References

1. F. A. Yassin, F. Y. El Kady, H. S. Ahmed, L. K. Mohamed, S. A. Shaban, A. K. Elfadaly, Highly effective ionic liquids for biodiesel production from waste vegetable oils. *Egyptian Journal of Petroleum* 24, 2015, 103
2. P. Koli, Photo galvanic cells: only solar cells having dual role of solar power generation and storage, *WIREs Energy and Environment* 7, 2018, e274.

3. A.K. Jana, Solar cells based on dyes. *Journal of Photochemistry and Photobiology A: Chemistry* 132, 2000, 1.
4. S. A. Mahmoud, H. Atia, S. H. Bendary, Synthesis of a high efficiency novel working electrode scandium/HOMBIKAT in dye-sensitized solar cells, *Solar Energy* 134, 2016 ,452.
5. S. A. Mahmoud, S. H. Bendary, H. Atia, A. Martin, Effect of Different Electrolytes on the Efficiency of Dye Sensitized Solar Cells for Solar Energy Conversion. *Journal of Nanoscience and Nanotechnology* 17, 2017, 3719.
6. S. A. Mahmoud, S. H. Bendary, A. A. Salem, O. A. Fouad, Facile synthesis of high yield two-dimensional zinc vanadate nanoflakes. *SN Applied Sciences* 1:497, 2019.
7. S.A. Mahmoud, B. S. Mohamed, Study on the Performance of Photogalvanic Cell for Solar Energy Conversion and Storage, *International Journal of Electrochemical Science* 10, 2015, 3340.
8. E. Rabinowitch, The Photogalvanic Effect I. The Photochemical Properties of the Thionine-Iron System. *The Journal of Chemical Physics* 8,1940, 551.
9. E. Rabinowitch, The photogalvanic effect II. The photogalvanic properties of the thionine-iron system. *The Journal of Chemical Physics* 8,1940 ,560.
10. K.R. Genwa, M.Genwa ,Photogalvanic cell: A new approach for green and sustainable chemistry. *Sol Energy Mater Sol Cells* 92, 2008,522.
11. K.M. Gangotri, R.C. Meena, R. Meena, Use of micelles in photogalvanic cells for solar energy conversion and storage: cetyl trimethyl ammonium bromide-glucose-toluidine blue system. *Journal of Photochemistry and Photobiology A: Chemistry* 123, 1999,93.
12. P. Wasserscheid, T. Wellton, *Ionic Liquids in Synthesis*, Wiley-VHC, New York, USA 2003
13. K.R. Genwa and C.Anju. Optimum efficiency of photogalvanic cell for solar energy conversion and storage containing Brilliant Black PN-Ammonium lauryl Sulphate –EDTA system. *Research Journal of Recent Sciences* 1 ,2012,117.
14. W.J.Albery, Development of photogalvanic cells for solar-energy conversion. *Accounts of Chemical Research* 15,1982,142.
15. W.J.Albery, M.D.Archer, Photogalvanic cells, potential of zero current. *Electrochimica Acta* 21, 1976,1155.
16. W.J.Albery, M.D.Archer, Optimum efficiency of photogalvanic cells for solar-energy conversion. *Nature* 270,1977,399.
17. A. Konno, G. R. A. Kumara, R. Hata, Effect of Imidazolium Salts on the Performance of Solid-state Dye-sensitized Photovoltaic Cell Using Copper Iodide as a Hole Collector. *Electrochemistry* 70, 2002, 432.
18. P. Bonhote, A. -P. Dias, N. Papageorgiou, K. Kalyanasundaram, M. Grätzel, Hydrophobic, Highly Conductive Ambient-Temperature Molten Salts, *Inorganic Chemistry* 35,1996, 1168.
19. W. Kubo, K. Murakoshi, T. Kitamura, S. Yoshida, M. Haruki, K.Hanabusa, H. Shirai, Y. Wada, S. Yanagida, Quasi-Solid-State Dye-Sensitized TiO<sub>2</sub> Solar Cells: Effective Charge Transport in

- Mesoporous Space Filled with Gel Electrolytes Containing Iodide and Iodine. *The Journal of Physical Chemistry B* 105, 2001, 12809.
20. W. Kubo, T. Kitamura, K. Hanabusa, Y. Wada, S. Yanagida, Quasi-solid-state dye-sensitized solar cells using room temperature molten salts and a low molecular weight gelator. *Chemical Communications* 4,2002, 374.
  21. J. Kruger, R. Plass, L. Cevey, M. Piccirelli, M. Grätzel, U. Bach, High efficiency solid-state photovoltaic device due to inhibition of interface charge recombination. *Applied Physics Letters* 79, 2001, 2085.
  22. M. Eisengerg, H.P. Silverman, Photo-electrochemical cells. *Electrochimica Acta* 5 ,1961, 1.
  23. A.S.N. Murthy, K.S. Reddy, in: *Proceedings of the International Solar Energy Conference, New Delhi, 1978*, 47.
  24. T. Yamse, Production of hydrogen by a photogalvanic cell with a flavin mononucleotide-EDTA system. *Photochemistry and Photobiology* 34 ,1981, 111.
  25. S.C. Ameta, R. Khamesra, K.M. Gangotri, S. Seth, Micelle Induced Photovoltage Generation. *Zeitschrift für Physikalische Chemie (Leipzig)* 271 ,1990,427.
  26. S.C. Ameta, S. Khamesra, A.K. Chittora, K.M. Gangotri, Use of sodium lauryl sulphate in a photogalvanic cell for solar energy conversion and storage: Methylene blue-EDTA system. *International journal of Energy Research* 13,1989, 643.
  27. K.M.Gangotri, R.C.Meena, R.Meena, *Journal of Photochemistry and Photobiology A: Chemistry*123,1999,93.
  28. J. Wang, H. Yao, Y. Nie, L. Bai, X. Zhang and J. Li, Application of Iron-Containing Magnetic Ionic Liquids in Extraction Process of Coal Direct Liquefaction Residues. *Industrial & Engineering Chemistry Research* 51 ,2012, 3776.
  29. P. Gangotri, K.M.Gangotri , Studies of the micellar effect on photogalvanics: solar energy conversion and storage in EDTA-safranin O-Tween-80 system. *Energy Fuel* 23,2009,2767.
  30. K.R.Genwa , A.Chouhan , Role of heterocyclic dye (Azur A) as a photosensitizer in photogalvanic cell for solar energy conversion and storage: NaLS-ascorbic acid system. *Solar Energy* 80, 2006,1213.
  31. S.Dube, S.L.Sharma, S.C.Ameta , Photogalvanic effect in Azur B-NTA system. *Energy Conversion and Management* 38,1997,101.
  32. K. Kalyanasundaram, Photo physics, photochemistry and solar energy conversion with tris(bipyridyl)ruthenium (II) and its analogues. *Coordination Chemistry Reviews.* 46 ,1982, 159.
  33. M. Montalti, A. Credi, L Prodi, MT Gandolfi, *Handbook of Photochemistry*, 3rd ed.; CRC Press: Boca Raton, FL, 2006.
  34. K. Nakamaru, Synthesis, luminescence quantum yields, and lifetimes of trischelated ruthenium(II) mixed-ligand complexes including 3,3'-dimethyl-2,2'-bipyridyl. *Bulletin of the Chemical Society of Japan.* 55 ,1982, 2697.
  35. A. J. Bard & M. A. Fox, *Artificial Photosynthesis: Solar Splitting of Water to Hydrogen and Oxygen.* *Accounts of Chemical Research* 28, 995,141.

36. [https://en.wikipedia.org/wiki/Tris \(bipyridine\) ruthenium \(II\) \\_chloride](https://en.wikipedia.org/wiki/Tris_(bipyridine)_ruthenium_(II)_chloride).
37. A. Juris, V. Balzani, F. Barigelletti, S. Campagna, P. Belser, A. von Zelewsky, Ru(II) polypyridine complexes: photophysics, photochemistry, electrochemistry, and chemiluminescence. *Coordination Chemistry Reviews* 84, 1988, 85.
38. S. Campagna, F. Puntoriero, F. Nastasi, G. Bergamini, V. Balzani, Photochemistry and photophysics of coordination compounds: Ruthenium. *Topics in Current Chemistry*. 280, 2007, 117.
39. Z. P. Wang, Z. M. Zhang, J. W. Zhang, X. Sun, Z. J. Ding, Luminescent properties of tris(2,2'-bipyridine) dichloro ruthenium(II) hexahydrate under high pressure, 248, 2011, 1106.
40. M. M. Richter, *Electrochemiluminescence (ECL)*, 104, 2004, 3003.
41. S. A. Mahmoud, B. S. Mohamed, M. Doheim, Ionic Liquid as Electrolyte in Photogalvanic Cell for Solar Energy Conversion and Storage. *International Journal of Energy and Power Engineering* 5, 2016, 203.

## Tables

**Table1: Influence of the variety of pH**

	pH					
Parameters	1.2	2	2.5	2.7	8	12
Photo potential (mV)	470	630	650	637	320	270
t(min)	37	32	36	31	30	30
Photocurrent ( $\mu A$ )	210	320	370	355	160.5	130
$P_{pp}$ ( $\mu W$ )	33.5	74.6	96.2	88.2	51.2	10.2
FF	0.34	0.37	0.4	0.39	0.31	0.29
$\eta\%$	0.63	1.4	1.9	1.7	0.98	0.19

[DATF] =  $6 \times 10^{-2}$  M; [OX] =  $1.9 \times 10^{-3}$  M; [TBRC] =  $4.1 \times 10^{-4}$  M; Pt electrode area  $0.5 \text{ cm}^2$ , light intensity =  $10 \times 4 \text{ mW cm}^{-2}$

**Table2: Influence of the variety in the concentration of photosensitizer dye**

Parameters	TRBC Conc., (M)				
	$4.1 \times 10^{-3}$	$3 \times 10^{-4}$	$3.5 \times 10^{-4}$	$4.1 \times 10^{-4}$	$4.6 \times 10^{-4}$
Photo potential (mV)	445	520	646	650	627
t(min)	31	33	35	36	37
Photocurrent ( $\mu A$ )	280	310	350	370	335
$P_{pp}$ ( $\mu W$ )	34.1	39.5	84.6	96.2	78.7
FF	0.34	0.35	0.38	0.4	0.36
$\eta\%$	0.71	0.95	1.5	1.9	1.8

[DATF] =  $6 \times 10^{-2}$  M; [OX] =  $1.9 \times 10^{-3}$  M; pH 2.5; Pt electrode area  $0.5 \text{ cm}^2$ , light intensity =  $10 \times 4 \text{ mW cm}^{-2}$

**Table3: Influence of the variety in the concentration of ionic liquid**

Parameters	DATF Conc., ( $\times 10^{-2}$ M)					
	2	3	4	6	8	9
Photo potential (mV)	570	620	640	650	590	470
t(min)	33	32	31	36	35	29
Photocurrent ( $\mu A$ )	305	330	348	370	312	245
$P_{pp}$ ( $\mu W$ )	43.2	75.6	84.1	96.2	54.5	32.5
FF	0.35	0.37	0.38	0.4	0.36	0.31
$\eta\%$	0.91	1.1	1.7	1.9	1.4	0.67

[TBRC] =  $1.4 \times 10^{-4}$  M; [OX] =  $1.9 \times 10^{-3}$  M; pH 2.5; Pt electrode area  $0.5 \text{ cm}^2$ ; light intensity =  $10 \times 4 \text{ mW cm}^{-2}$

**Table 4: Influence of the variety in the concentration of reductant**

OX Conc., ( $\times 10^{-3}$ M)						
Parameters	1	1.3	1.9	2.4	4	6
Photo potential (mV)	530	610	650	620	590	470
t(min)	29	33	36	34	35	29
Photocurrent ( $\mu A$ )	290	330	370	320	312	245
$P_{pp}$ ( $\mu W$ )	36.2	78.6	96.2	86.2	64.5	22.5
FF	0.35	0.36	0.4	0.37	0.36	0.29
$\eta\%$	0.88	1.5	1.9	1.6	1.3	0.77

[TBRC] =  $1.4 \times 10^{-4}$  M; [DATF] =  $6 \times 10^{-2}$  M; pH 2.5; Pt electrode area  $0.5 \text{ cm}^2$ ; light intensity =  $10 \times 4 \text{ mW cm}^{-2}$

**Table 5: output parameters of PGC system**

PGC system TBRC Conc., $4.1 \times 10^{-3}$ , CATF Conc., $2.5 \times 10^{-3}$ , OX conc., $1.9 \times 10^{-3}$ , pH 2.5, Pt electrode area $0.5 \text{ cm}^2$ & light intensity = $10.4 \text{ m cm}^{-2}$					
Parameter	photo potential (mV)	Photocurrent ( $\mu A$ )	$P_{pp}$ ( $\mu W$ )	FF	$\eta\%$
	650	370	96.2	0.4	1.9

## Figures

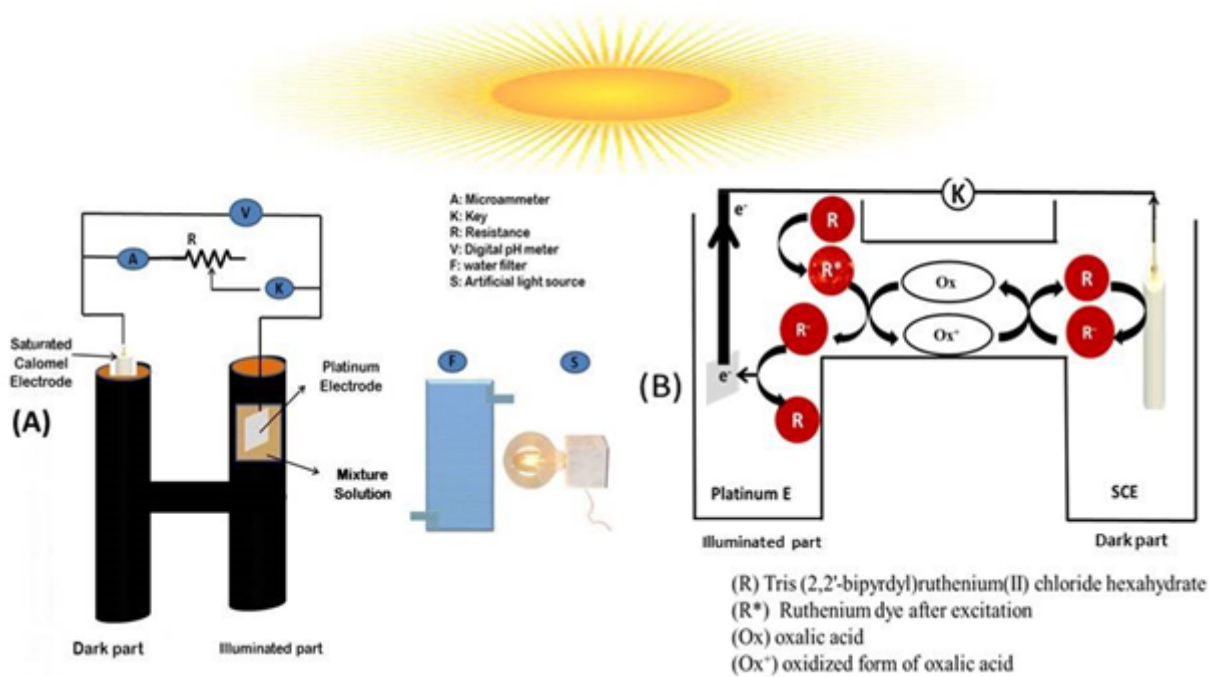


Figure 1

(A) photogalvanic cell parts. (B) Mechanism technique for PG working

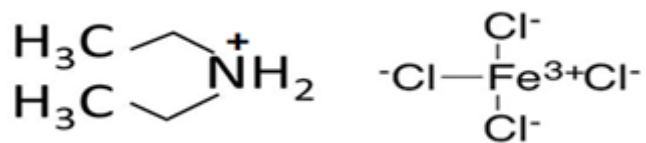


Figure 2

Diethyl ammonium tetrachloro ferrate

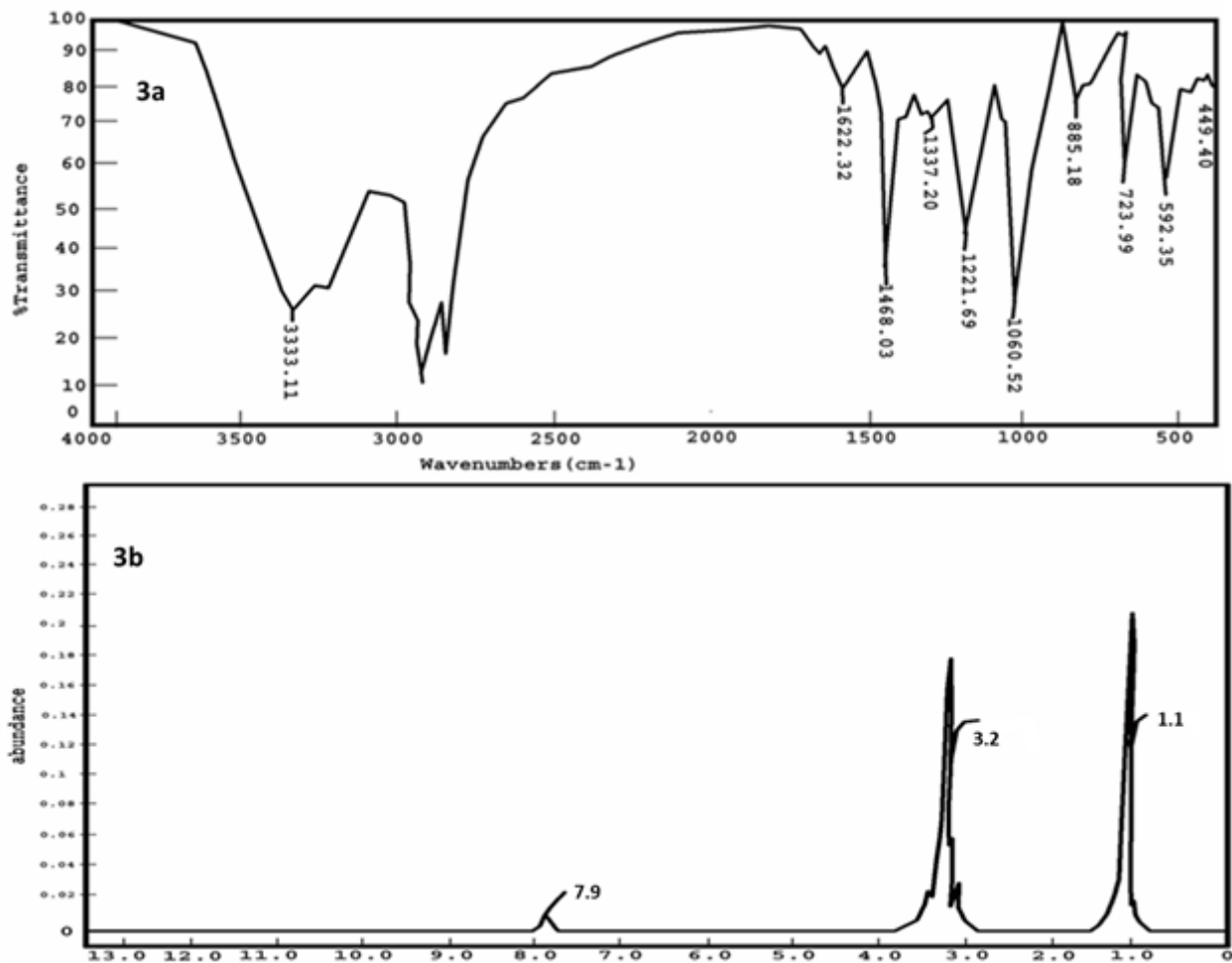


Figure 3

3A FTIR & 3B HNMR spectra of Diethyl ammonium tetrachloro ferrate

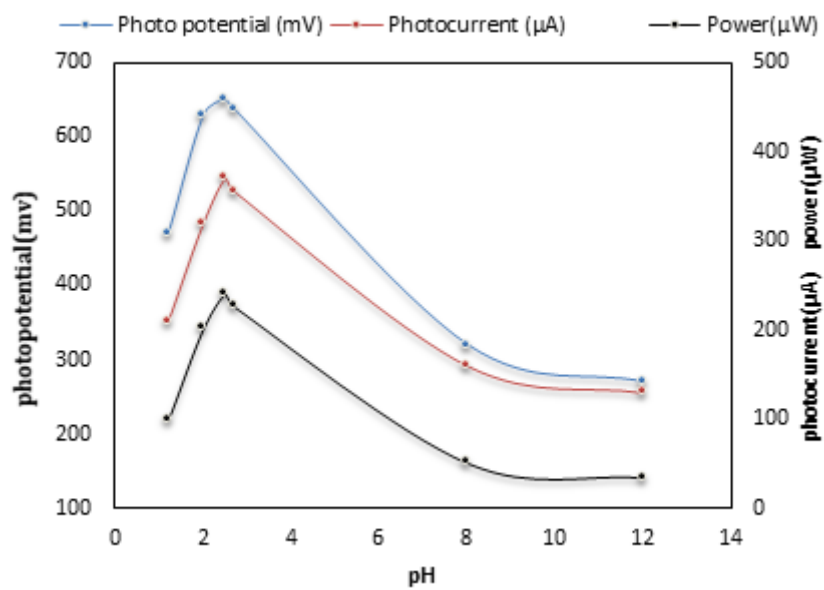


Figure 4

Variation of the pH; Potential, Current and power vs. pH

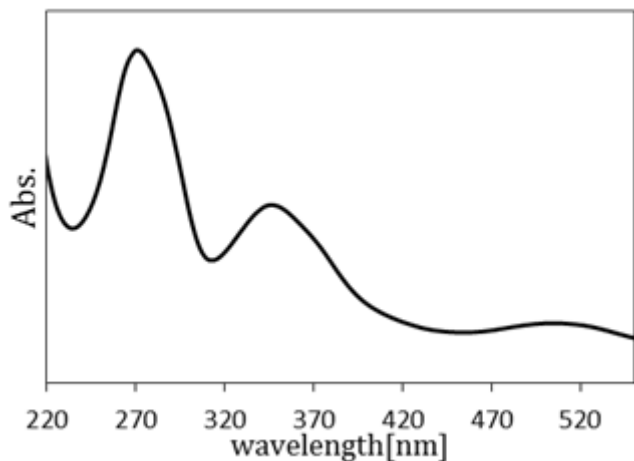


Figure 5

UV spectra of TBRC

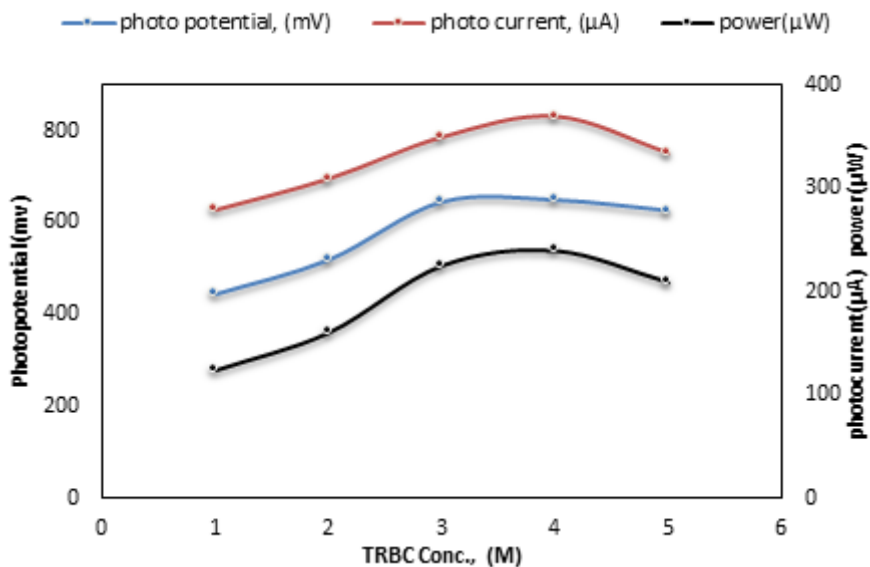


Figure 6

Variation of the Dye; Potential, Current and power vs. Concentration.

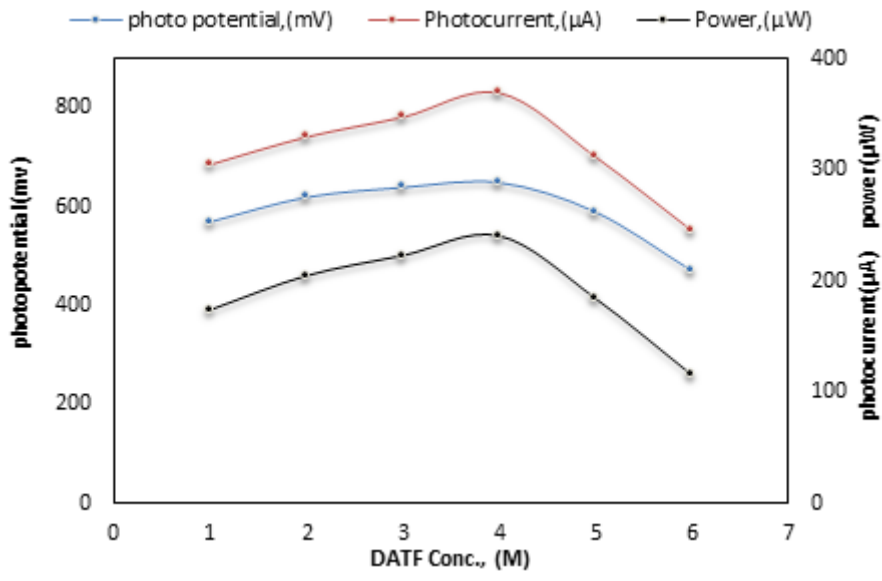


Figure 7

Variation of the Ionic liquid [DATF]; Potential, Current and power vs. Concentration.

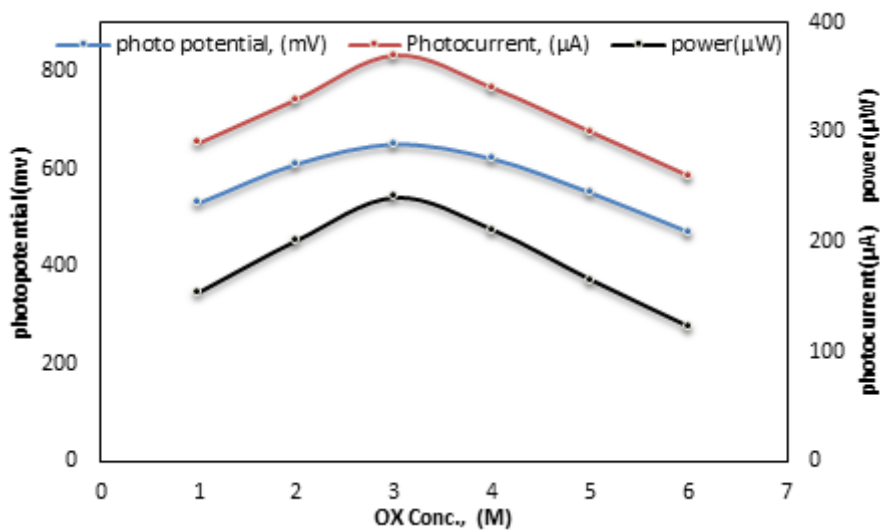


Figure 8

Variation of the Oxalic acid reductant; Potential, Current and power vs. Concentration

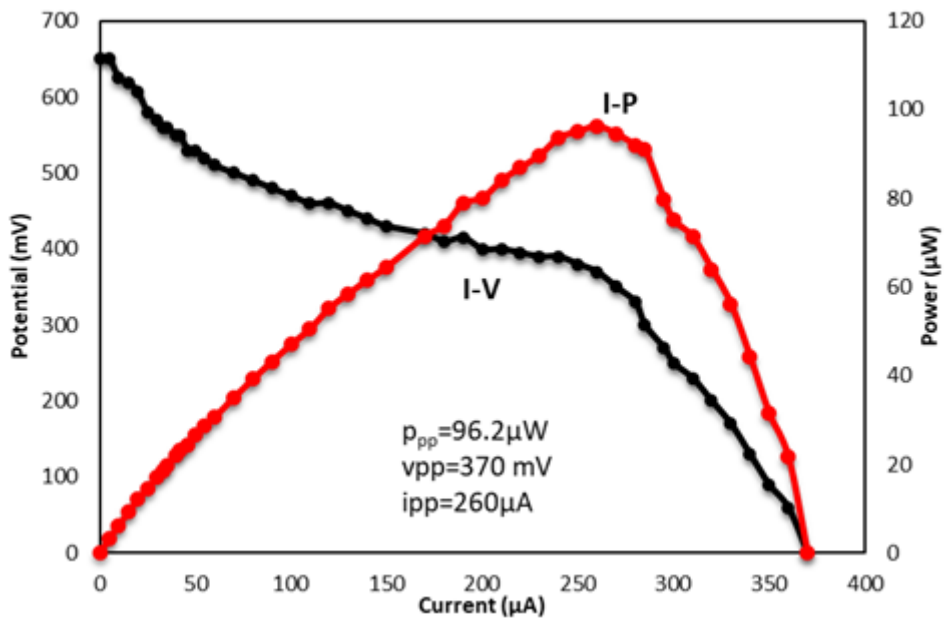


Figure 9

Variation of the potential and power with the i-V characteristics of the cell. (1) Potential vs. current(I-V) , (2) Power vs. current a(I-P)

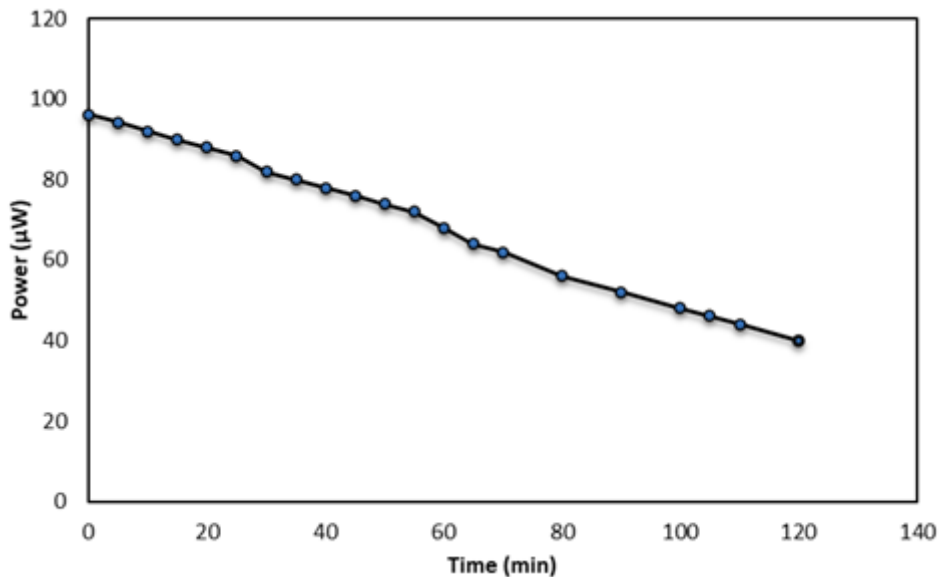


Figure 10

Storage capacity of the cell (retrieval of the stored power in dark from the cell).

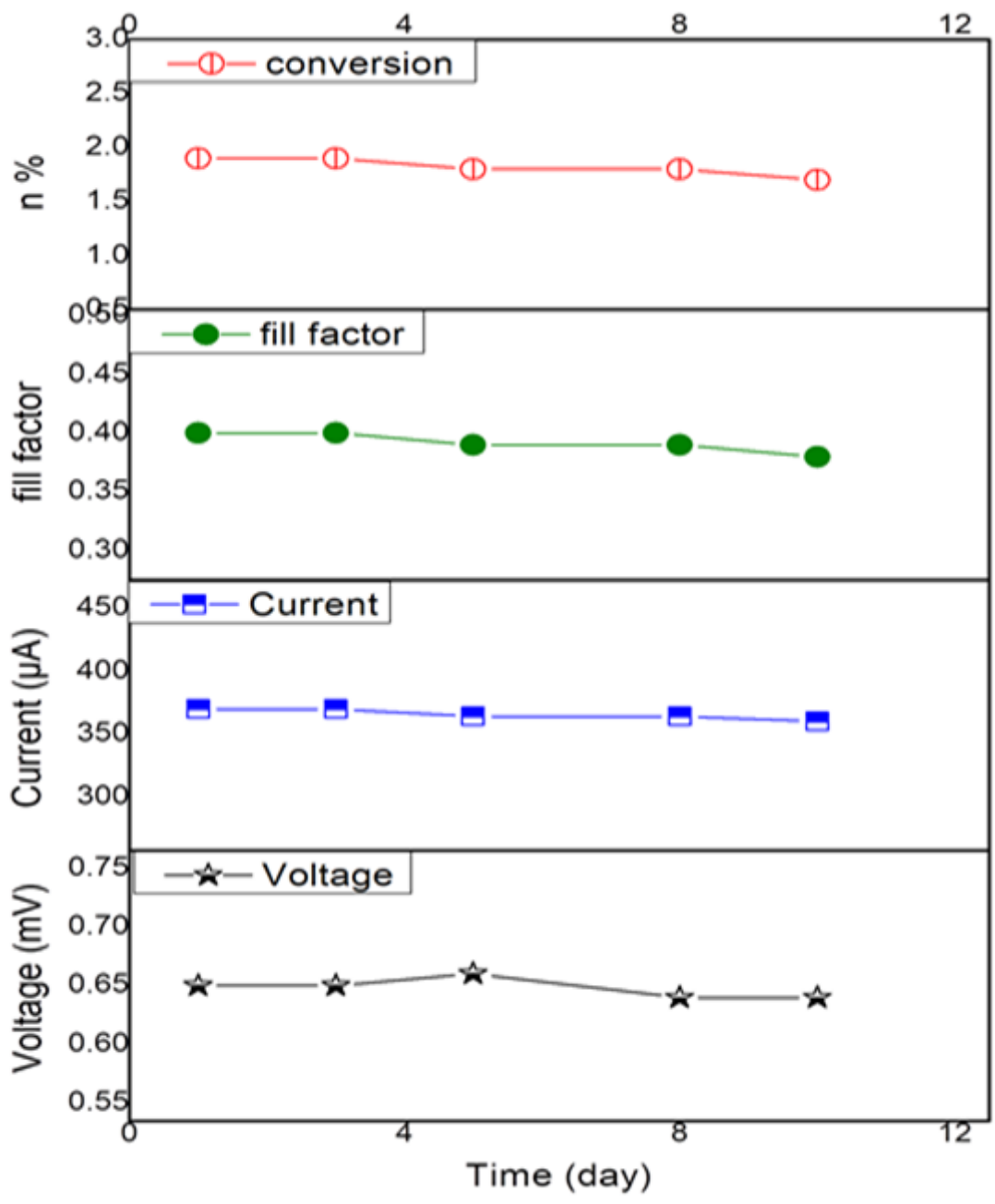


Figure 11

Stability test of PGC at different time